Turkish Journal of Physics

Volume 41 | Number 4 Article 6

1-1-2017

Achieving carrier and photon confinement in Ga(NAsP)/AlGaP/GaP QWs on Si substrates

ÖMER LÜTFİ ÜNSAL

BEŞİRE GÖNÜL

Follow this and additional works at: https://journals.tubitak.gov.tr/physics

Part of the Physics Commons

Recommended Citation

ÜNSAL, ÖMER LÜTFİ and GÖNÜL, BEŞİRE (2017) "Achieving carrier and photon confinement in Ga(NAsP)/AlGaP/GaP QWs on Si substrates," *Turkish Journal of Physics*: Vol. 41: No. 4, Article 6.
https://doi.org/10.3906/fiz-1703-25
Available at: https://journals.tubitak.gov.tr/physics/vol41/iss4/6

This Article is brought to you for free and open access by TÜBİTAK Academic Journals. It has been accepted for inclusion in Turkish Journal of Physics by an authorized editor of TÜBİTAK Academic Journals. For more information, please contact academic.publications@tubitak.gov.tr.

Turkish Journal of Physics

http://journals.tubitak.gov.tr/physics/

Research Article

Turk J Phys
(2017) 41: 337 – 343
© TÜBİTAK
doi:10.3906/fiz-1703-25

Achieving carrier and photon confinement in Ga(NAsP)/AlGaP/GaP QWs on Si substrates

Ömer Lütfi ÜNSAL*, **Beşire GÖNÜL**
Department of Engineering of Physics, Faculty of Engineering, Gaziantep University, Gaziantep, Turkey

Received: 21.03.2017 • **Accepted/Published Online:** 29.05.2017 • **Final Version:** 05.09.2017

Abstract: A detailed comparative theoretical analysis on both carrier and photon confinement of dilute nitride direct bandgap $GaN_xAs_{1-x-y}P_y$ with that of $GaAs_{1-y}P_y$ on Si substrates is presented. Model calculations indicate that optical confinement factor of $GaAs_{1-y}P_y$/GaP is greater than that of $GaN_xAs_{1-x-y}P_y$/GaP for all concentrations. We have demonstrated that one can improve the optical confinement factor of $GaN_xAs_{1-x-y}P_y$/GaP by using an $Al_zGa_{1-z}P$ cladding layer.

Key words: Dilute nitride phosphide alloys, N incorporation, effective mass, band anticrossing model, carrier and photon confinement

1. Introduction

The never-ending quest to find easy to manufacture, efficient, and cost effective optoelectronic devices that would satisfy the need for high performance devices operating in the optical telecommunication wavelength range of 1.3 μm has brought us to GaP-based III-N-V material systems. GaP-based $GaAs_{1-y}P_y$ alloys have found applications in optoelectronic devices for a long time, and as a result the physical properties of these alloys such as atomic structure, energy band structure, and effective mass have been studied in great detail. However, the lack of suitable substrate leading to $GaAs_{1-y}P_y$ alloys to be grown on GaP substrates causes problems such as lattice mismatch [1], matching refractive index, and poor band structure configuration [2], which yield decreased layer thickness, poor carrier and optical confinement, and reduced electron effective mass [3]. With the incorporation of nitrogen (N) into $GaAs_{1-y}P_y$ alloy, these physical properties have been changed significantly and these major challenges are overcome [4]. Arsenide (As)-rich dilute nitride Ga(NAsP) is lattice matched to GaP and hence Si substrates with a direct band gap [5,6].

The primary and important factor of designing a semiconductor quantum well laser is the confinement of both carrier and optical mode. Confinement of carriers is ultimately determined by the band offset design of the heterostructures. Optical mode is related to the refractive index difference between the active layer and cladding layer of the waveguide. It is known that the refractive index strongly depends on the direct band gap of the semiconductor materials and the band gap of III-V semiconductor material system can be modified by means of incorporating nitrogen into the host semiconductor GaAsP. In this paper, we present the results of comparative theoretical analysis of carrier and photon confinement by determining electronic band offsets, refractive indices of the heterostructures, and corresponding optical confinement factors of the proposed III-N-V laser material systems Ga(NAsP) with an AlGaP cladding layer on Si substrates.

*Correspondence: omerlutfiunsal@gmail.com

The paper is organized as follows. The material composition that yields the optimum band configuration of Ga(NAsP) is presented in Section 2. The concentration dependence of optical confinement and its comparison with the host matrix $GaAs_{1-y}P_y$ are studied in Section 3. Our conclusions are presented in Section 4. Required theoretical models are presented in each of the related sections.

2. The modelling of the band structure of $GaAs_{1-y}P_y$ and $GaN_xAs_{1-x-y}P_y$

For a well-designed optoelectronic material, the structure and form of its band alignment is an important factor. The band alignment is defined by band discontinuity between the active layer and barrier and the distribution of this discontinuity over relative bands. The distributed discontinuity of conduction and valance bands are represented as ΔE_c and ΔE_v, respectively. Physical properties of the constituent semiconductor alloys characterize how the band discontinuity is generated. It has been shown that incorporating N into Ga(NAsP) affects its conduction band states, which leads to an increase in conduction band offset Q_c, and a small discontinuity in the valence band edge [7]. In accord with Van de Walle's model solid theory [8] the band offset ratio for conduction and valence band, $Q_{c,v}$, is determined by discontinuity fractions of $\Delta E_c/\Delta E_g$. The energy of the potential barrier, ΔE_g, is determined from the difference between the bulk bandgap energy of barrier layers and strained bandgap energy of the active layer. Conduction band edge energy can be found by adding strained bandgap to the valence band edge energy, which is chosen as zero. The valence band edge energy is

$$E_v(x,y) = \begin{cases} E_{v,av}(x,y) + \frac{\Delta_0(x,y)}{3} + \delta E_{hh}(x,y) \text{ for } hh \text{ (compressive strain)} \\ E_{v,av}(x,y) + \frac{\Delta_0(x,y)}{3} + \delta E_{lh}(x,y) \text{ for } lh \text{ (tensile strain)} \end{cases}, \quad (1)$$

where $E_{v,av}(x,y)$ is average energy of valence band and Δ_0 is energy of spin-orbit split-off band. Table 1 provides all the related parameters. The shift in conduction band energy can be calculated as

$$\delta E_c(x,y) = 2a_c\left(1 - \frac{C_{12}}{C_{11}}\right)\varepsilon \quad (2)$$

Table 1. Material parameters of binary compounds used in our calculations, taken from Vurgaftman et al. [9].

Material	AlP	GaAs	GaP	GaN
a_0 (Å)	5.467	5.6532	5.4504	4.5
E_o (eV)	3.56	1.424	2.777	3.299
Δ_0 (eV)	0.07	0.341	0.08	0.017
(m_e^*, Γ)	0.22	0.067	0.13	0.15
(m_e^*, SO)	0.30	0.172	0.25	0.29
γ_1	3.35	6.98	4.05	2.67
γ_2	0.71	2.06	0.49	0.75
γ_3	1.23	2.93	2.93	1.10
n (λ_g)[10]	3.0	3.6	3.4	2.6
a_c (eV)	–5.7	–7.17	–8.2	–2.2
a_v (eV)	–3.0	–1.16	–1.7	–5.2
$E_{v,av}$	–8.09	–6.92	–7.40	×
b (eV)	–1.5	–2.0	–1.6	–2.2
C_{12} (GPa)	630.0	566.0	620.3	159.0
C_{44} (GPa)	615.0	600.0	703.3	155.0

The valance bands are shifted by the energy $\delta E_{hh}(x,y)$ and $\delta E_{lh}(x,y)$:

$$\delta E_{hh}(x,y) = -P_\varepsilon - Q_\varepsilon$$

$$\delta E_{lh}(x,y) = -P_\varepsilon + Q_\varepsilon, \tag{3}$$

where

$$P_\varepsilon = -2a_v \left(1 - \frac{C_{12}}{C_{11}}\right)\varepsilon$$

$$Q_\varepsilon = -b\left(1 + \frac{2C_{12}}{C_{11}}\right)\varepsilon, \tag{4}$$

and where a_c and a_v are the conduction- and valance-band hydrostatic deformation potentials, b is the valance band shear deformation potential, and C_{11} and C_{12} are elastic stiffness constants. The strained band gaps can be expressed as

$$E_{c-hh}(x,y) = E_g(x,y) + \delta E_c(x,y) - E_{hh}(x,y)$$

$$E_{c-lh}(x,y) = E_g(x,y) + \delta E_c(x,y) - E_{lh}(x,y), \tag{5}$$

The conduction band position is

$$E_c(x,y) = \begin{cases} E_v(x,y) + E_{c-hh}(x,y) \ \text{ for } hh \ \text{(compressive strain)} \\ E_v(x,y) + E_{c-lh}(x,y) \ \text{ for } lh \ \text{(tensile strain)} \end{cases} \tag{6}$$

$$\frac{\Delta Ec}{\Delta Eg} = 1 - \frac{E_v^w - E_v^b}{E_g^b - E_g^w}, \tag{7}$$

where E_v^w and E_v^b are valance band positions in well and barrier materials, respectively, and E_g^w and E_g^b are strain adjusted band gaps for active layer and barrier materials.

Figure 1a presents the calculated band offset ratios of Q_c and Q_v for compressively strained $GaAs_{1-y}P_y$ and As-rich $GaN_xAs_{1-x-y}P_y$ type I quantum well with GaP barriers on Si substrates. A closer investigation of Figure 1a shows clearly that incorporation of N into $GaAs_{1-y}P_y$ provides an improvement for band alignment configuration. Conduction band offset ratio Q_c for $GaAs_{1-y}P_y$ is less than its valance band offset ratio Q_v, which causes the band offset energy of the conduction band ΔE_c to be less than the valance band offset energy ΔE_v. This is an undesired band alignment structure that may cause an electron spill out to the barriers. By incorporating N into $GaAs_{1-y}P_y$, band alignment is improved substantially.

The calculations presented in Figures 1a and 1b show distinctly the improvement in band alignment due to incorporation of N into host matrix $GaAs_{1-y}P_y$. With the incorporation of N into $GaAs_{1-y}P_y$, valance band offset ratio Q_v is now less than conduction band offset ratio Q_c. This will in turn increase Q_c and decrease Q_v gradually. For the corresponding band offset energies of ΔE_c and ΔE_v, one can see that there is a significant development of band alignment in $GaN_xAs_{1-x-y}P_y$ compared to that of the host matrix $GaAs_{1-y}P_y$. This development is achieved with a higher nitrogen and a lower phosphide concentration in $GaN_xAs_{1-x-y}P_y$. Larger ΔE_c, in turn, yields an improved confinement condition for electrons in wells and

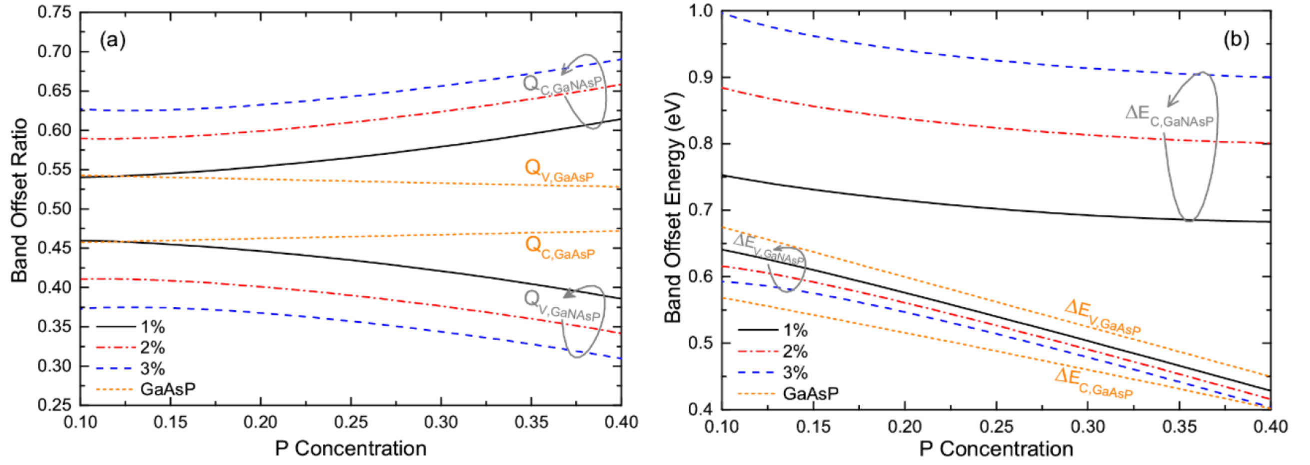

Figure 1. Variation in (a) band offset ratio of Q_c and Q_v and (b) band offset energies of ΔEc and ΔEv in $GaN_xAs_{1-x-y}P_y$/GaP QW on Si substrate as a function of phosphide and nitrogen concentration.

effectively decreases the electron spill out. This is due to incorporated N that mainly affects conduction band energy states. As a result, the incorporation of nitrogen into $GaAs_{1-y}P_y$ mainly affects conduction band offset energy and there are only minor changes in valence band offset energy. Overall, an ideal band alignment of deep conduction- and shallow valence-wells can be achieved in $GaN_xAs_{1-x-y}P_y$ /GaP structure with a lower phosphide concentration.

3. Five-layer symmetric slab modelling and results

The obtained laser light should be confined in the heterostructure. For this aim different type waveguides have been produced. One of these waveguides is five-layer slab waveguide [11] and so we performed our calculations according to this waveguide type. The structure is shown in Figure 2.

Using the five-layer slab waveguide method, optical confinement factor can be obtained as

$$v^2 = a^2k^2\left(n_1^2 - n_3^2\right) \tag{8}$$

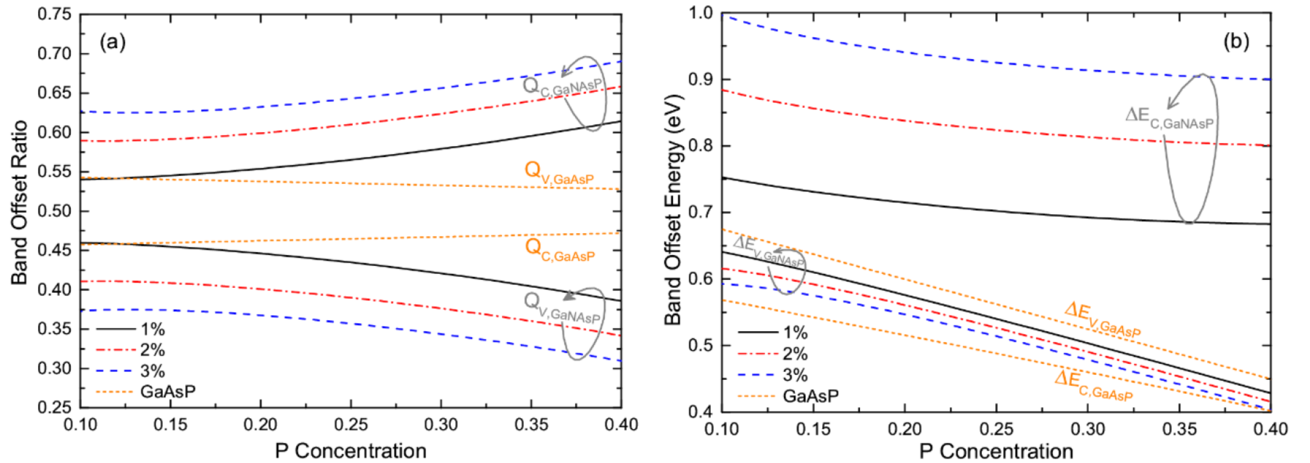

Figure 2. Illustration of the five-layer slab waveguide.

$$u^2 = a^2\left(k^2n_1^2 - \beta^2\right) = a^2h_1^2 \tag{9}$$

$$w^2 = a^2\left(\beta^2 - k^2n_3^2\right) = v^2 - u^2 = a^2h_3^2 \tag{10}$$

$$t^2 = a^2\left(k^2n_2^2 - \beta^2\right) = u^2 - v^2c^2 = a^2h_2^2 \tag{11}$$

$$t''^2 = a^2\left(\beta^2 - k^2n_2^2\right) = v^2c^2 - u^2 = a^2h_2''^2 \tag{12}$$

$$c = \frac{n_1^2 - n_2^2}{n_1^2 - n_3^2} \approx \frac{n_1 - n_2}{n_1 - n_3} \tag{13}$$

$$u = M\pi + \arctan\left(\frac{t}{u}\tan\left(\arctan\left(\frac{w}{t}\right) - t\left(\frac{b}{a} - 1\right)\right)\right) \tag{14}$$

If $t \to it''$

$$u = M\pi + \arctan\left(\frac{t''}{u}\tanh\left(\operatorname{arctanh}\left(\frac{w}{t''}\right) - t''\left(\frac{b}{a} - 1\right)\right)\right) \tag{15}$$

If $c \leq u/v \leq 1$;

$$\Gamma = \frac{u + \sin u \cos u}{u + \sin u \cos u\left(1 - \frac{u^2}{t^2}\right) + u\left(\cos^2 u + \frac{u^2}{t^2}\sin^2 u\right)\left(\frac{b}{a} - 1 + \frac{1}{w}\right)} \tag{16}$$

If $0 \leq u/v \leq c$;

$$\Gamma = \frac{u + \sin u \cos u}{u + \sin u \cos u\left(1 - \frac{u^2}{t''^2}\right) + u\left(\cos^2 u + \frac{u^2}{t''^2}\sin^2 u\right)\left(\frac{b}{a} - 1 + \frac{1}{w}\right)} \tag{17}$$

The concentration dependence of refractive indices of well- and cladding layer material are given in Table 2 for different concentrations. Table 2 indicates that refractive index of $GaN_xAs_{1-x-y}P_y$ decreases with N concentration. To satisfy and improve the conditions of internal reflection for the five-layer slab waveguide shown in Figure 2, the refractive index of the $GaN_xAs_{1-x-y}P_y$ layer, which is denoted as n_1, must be greater than that of the barrier and cladding layer, which are denoted as n_2 and n_3, respectively. To achieve better internal reflection, the refractive index of the cladding layer should be minimized. Thus, the incorporation of Al into GaP and use of $Al_zGa_{1-z}P$ as a cladding layer can be offered as a solution. The choice of $Al_zGa_{1-z}P$ as a cladding layer can cause a decrease in the refractive index without adding strain to the material system due to insignificant lattice mismatch between AlP and GaP.

Table 2. Refractive index for $GaN_xAs_{0.8-x}P_{0.2}$ and $Al_zGa_{1.0-z}P$.

Content	x (%)	1%	2%	3%	4%
	$GaN_xAs_{0.8-x}P_{0.2}$	3.514	3.474	3.438	3.407
	z (%)	5%	10%	15%	20%
	$Al_zGa_{1.0-z}P$	3.380	3.360	3.340	3.320

We assume a total loss of 50 cm^{-1} for the Fabry Perot laser cavity. The cavity length L is taken as 1500 μm. In comparison to the refractive index of GaAs and GaP, the refractive index of GaN is much

smaller. Therefore, introduction of N into host material $GaAs_{1-y}P_y$ causes an undesired decrease in refractive index of $GaN_xAs_{1-x-y}P_y$ QW. Hence, the index difference between $GaN_xAs_{1-x-y}P_y$ well and GaP barrier decreases as well. This reduced index difference between well and barrier is expected to cause a decrease in optical confinement factor, Γ. In order to improve Γ, a cladding layer of $Al_zGa_{1-z}P$ is suggested. The most important advantage of $Al_zGa_{1-z}P$ as a cladding layer is being lattice-matched to Si substrate in the Ga(NAsP)/GaP material system. Thus, the waveguide model is employed to investigate the optical confinement factor [11] for Ga(NAsP)/GaP/$Al_zGa_{1-z}P$. All required parameters are provided in Table 1.

Figure 3a compares the rate of change in the optical confinement factor of the two proposed 70 Å single QW laser systems of $GaAs_{1-y}P_y/GaP/Al_{0.3}Ga_{0.7}P$ and $GaN_xAs_{1-x-y}P_y/GaP/Al_{0.3}Ga_{0.7}P$ on Si substrates. We first try to show phosphide concentration dependence of Γ for the two QW systems taking the index of refraction of active, barrier, and cladding layers at each composition into account. We choose the aluminum concentration in the confining layer as 30% in both systems. As can be seen from Figure 3a, the $GaAs_{1-y}P_y/GaP/Al_{0.3}Ga_{0.7}P$ material system has a higher confinement factor than that of $GaN_xAs_{1-x-y}P_y/GaP/Al_{0.3}Ga_{0.7}P$. This is due to GaN having a much smaller refractive index than other constituent binary compounds. In addition, an increase in phosphide concentration reduces Γ in both systems as GaAs have the largest refractive index in the material composition, and therefore any reduction in As concentration results in a lower refractive index for the active layer. Secondly, these calculations show clearly how Γ decreases with increasing nitrogen concentration for the $GaN_xAs_{1-x-y}P_y/GaP/Al_{0.3}Ga_{0.7}P$ material system. Thus, an increase in nitrogen and phosphide concentration in the well leads to a poor photon confinement in $GaN_xAs_{1-x-y}P_y/GaP/Al_{0.3}Ga_{0.7}P$. However, increasing the Al concentration in the cladding layer, $Al_zGa_{1.0-z}P$, the optical confinement factor can be improved substantially. As seen in Figure 3b the optical confinement factor of $GaN_xAs_{1-x-y}P_y/GaP/Al_{0.3}Ga_{0.7}P$ increases with Al concentration and its value approaches that of $GaAs_{0.9}P_{0.1}$, showing promising properties as far as the optical confinement factor is concerned.

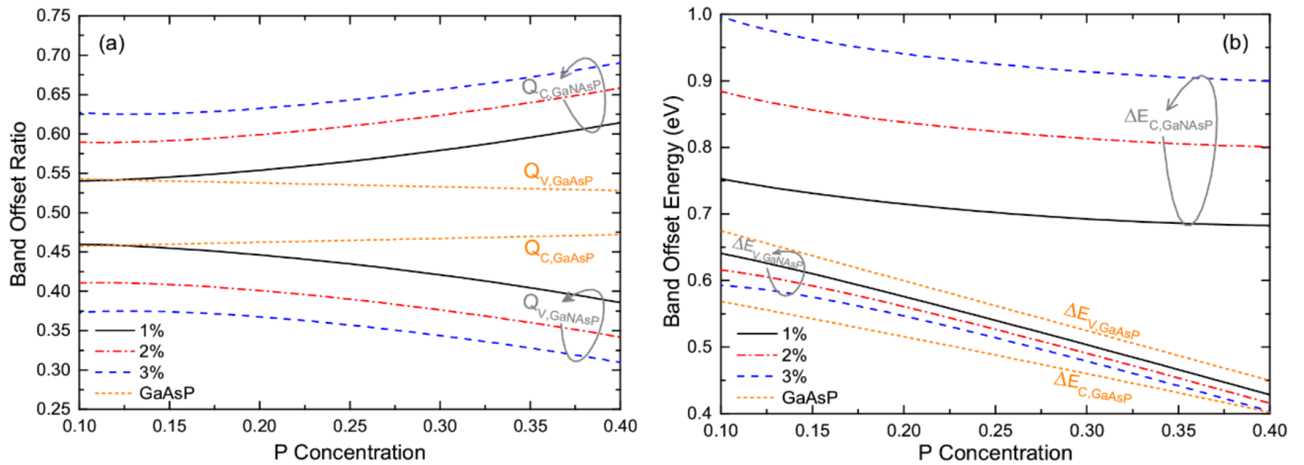

Figure 3. (a) The calculated values of Γ as a function of phosphide concentration in well for $GaAs_{1-y}P_y/GaP/Al_{0.3}Ga_{0.7}P$ and $GaN_xAs_{1-x-y}P_y/GaP/Al_{0.3}Ga_{0.7}P$. (b) The variation of Γ versus aluminum concentration in cladding layer for $GaAs_{0.9-y}P_y/GaP/Al_zGa_{1-z}P$ and that of $GaN_xAs_{0.9-x}P_{0.1}/GaP/ Al_zGa_{1-z}P$. The nitrogen concentration is varied between 1% and 4% for the quaternary system.

4. Summary and conclusions

We have made a comprehensive theoretical comparative analysis of carrier and photon confinement properties in $GaAs_{1-y}P_y/GaP/Al_zGa_{(1-z)}P$ and $GaN_xAs_{1-x-y}P_y/GaP/Al_zGa_{(1-z)}P$ laser systems on Si substrates.

Using model solid theory on the $GaN_xAs_{1-x-y}P_y/GaP$ material system, band offset energies and ratios are calculated. The results indicate that conduction band offset energy increases in leaps with the addition of small percentages of N, removing the problem of carrier leakage in $GaAs_{1-y}P_y/GaP$ due to its poor band offset configuration. High As concentration in both material systems provides slightly larger conduction band offset energies but not as much as one could get from N incorporation. Even though band offset configuration and carrier confinement benefit from N incorporation, due to the low refractive index of GaN, optical confinement of the $GaN_xAs_{1-x-y}P_y/GaP$ laser system is slightly worse than that of $GaAs_{1-y}P_y/GaP$ laser systems while having an advantage on the strain levels over $GaAs_{1-y}P_y/GaP$ laser systems. However, introducing $Al_zGa_{(1-z)}P$ as a cladding layer to $GaN_xAs_{1-x-y}P_y/GaP$ heterojunction, the optical confinement factor can be improved substantially. In summary, significant improvements in the aspects of carrier and photon confinement are shown for the compressively strained laser system of $GaN_xAs_{1-x-y}P_y/GaP/Al_zGa_{(1-z)}P$.

Acknowledgment

This work was supported by the Scientific and Technological Research Council of Turkey (TÜBİTAK) under Grant No. 113F407.

References

[1] Jin, X.; Fuchi, S.; Takeda, Y. *J. Cryst. Growth* **2013**, *370*, 204-207.

[2] Abramkin, D. S.; Putyato, M. A.; Budennyy, S. A.; Gutakovskii, A. K.; Semyagin, B. R.; Preobrazhenskii, V. V.; Kolomys, O. F.; Strelchuk, V. V.; Shamirzaev, T. S. *J. Appl. Phys.* **2012**, *112*, 083713.

[3] Wetzel, C.; Meyer, B. K.; Omling P. *Phys. Rev. B.* **1993**, *47*, 15588.

[4] Ünsal, Ö. L.; Gönül, B. *Physica E.* **2016**, *80*, 176-184.

[5] Kunert, B.; Volz, K.; Koch, J.; Stolz, W. *Appl. Phys. Lett.* **2006**, *88*, 182108.

[6] Ünsal, Ö. L.; Gönül, B.; Temiz, M. *Chinese Physics B.* **2014**, *23*, 077104.

[7] Minch, J.; Park, S. H.; Keating, T.; Chuang, S. L. *IEEE J. Quantum Electron.* **1999**, *35*, 771.

[8] Van de Walle, C. G. *Physical Review B.* **1989**, *39*, 1871.

[9] Vurgaftman, I.; Meyer J. R. *J. Appl. Phys.* **2003**, *94*, 3675-3696.

[10] Kasap, S.; Capper, P. *Handbook of Electronic and Photonic Materials*, Springer: New York, NY, USA, 2007.

[11] Adams, M. J. *An Introduction to Optical Waveguides*, John Wiley & Sons: Hoboken, NJ, USA, 1981, pp. 82-86.